SAND95-1087C

An 'Exact' Treatment of Self-Shielding and Covers in Neutron Spectra Determinations[1]

Conf-950716--2

Patrick. J. Griffin and John G. (Jake) Kelly
Sandia National Laboratories
Albuquerque, NM 87185

Abstract

Most neutron spectrum determination methodologies ignore self-shielding effects in dosimetry foils and treat covers with an exponential attenuation model. This work provides a quantitative analysis of the approximations in this approach. It also provides a methodology for improving the fidelity of the treatment of the dosimetry sensor response to a level consistent with the user's spectrum characterization approach. A library of correction functions for the energy-dependent sensor response has been compiled that addresses dosimetry foils/configurations in use at the Sandia National Laboratories Radiation Metrology Laboratory.

I. INTRODUCTION

Almost all nuclear facilities use activation foils to characterize the neutron spectrum from fission sources. Codes such as LSL-M2 [1] and SAND-II [2, 3] use the activation of dosimetry-quality reactions to "adjust" a trial spectrum, typically obtained from Monte Carlo calculational methods, or to "unfold" the spectrum. A necessary condition for a good spectral determination is a set of activation sensors that provides good energy coverage for the neutron spectrum [4] and that possesses very well-characterized and self-consistent cross sections [5]. Covers of cadmium, gold, gadolinium, and boron [4, 6] are often placed over dosimetry foils to shift the energy region of primary response in order to cover regions of the neutron spectrum that do not exhibit sufficient response to well-characterized easily fielded pure activation sensors. The word "sensor" in this paper refers to the complete deployed measuring system, that is the combination of dosimetry material (typically in the form of a foil, pellet, wire, or even a silicon transistor) and any cover material. The sensor response function is the energy-dependent characterization of the sensor output reading, typically proportional to a specific decay radiation (either a gamma ray or beta activity) read in a laboratory counting system, when the complete sensor is exposed to a neutron field with an fluence of 1 n/cm^2.

The detailed effects of the physical geometry of deployed sensors are seldom modeled. This paper (1) sets the background for an "exact" treatment by describing current modeling practices, (2) focuses the concern by comparing current practices with "exact" models, and (3) provides the dosimetry community with a methodology for computing "exact" response functions for commonly used sensor configurations that can be interfaced with standard spectrum determination codes. The results of this work are an improvement in the self-consistency of covered dosimetry sensors and the definition of an expanded set of sensors with better energy coverage that can be used for spectrum determinations. The tools used to produce these improved response functions and the details of the methodology are made available to the community to facilitate their application to site-specific sensor configurations.

II. SELF-SHIELDING

Self-shielding occurs when a "thick" sensor is used. In this case, the neutron flux can be artificially reduced by the outer regions of a sensor so that the sensor-averaged response, which is measured in the counting laboratory, is not representative of the actual neutron field. A measure of the importance of self-shielding is the ratio of the sensor cross section for an infinitely dilute material to the actual sensor-averaged cross section. Figures 1 and 2 show the energy-dependent values of this ratio for disk-shape gold foils of various thicknesses. The dosimetry reaction of interest is ^{197}Au(n,γ)^{198}Au; the foil diameter is representative of that for commercially available dosimetry-quality activation foils (~1.27 cm). The low energy and 4.9 eV depression in the correction factor are the result of self-shielding effects in areas of a large cross section. The resonance region and high energy enhancements are a result of the scattering effects that are discussed in Section III.

The self-shielding effect is not typically treated by any current spectrum determination methodology. It is, instead, avoided. In the case of gold, dilute foils are readily available. Figures 1 and 2 show the effect of various thicknesses of gold foil. However, these figures are for illustration only. Dilute gold foils should be used in the characterization of reactor spectra when-

[1]This work was performed at Sandia National Laboratories, which is operated for the U.S. Department of Energy under Contract DE-AC04-94AL85000.

DISCLAIMER

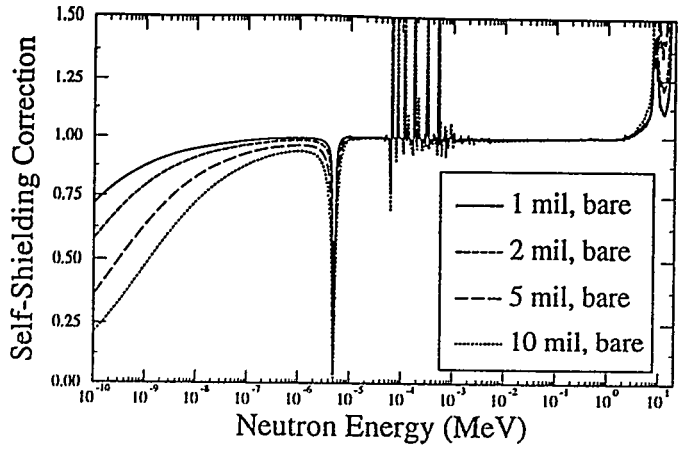

FIGURE 1. Importance of Self-Shielding in Gold Sensors

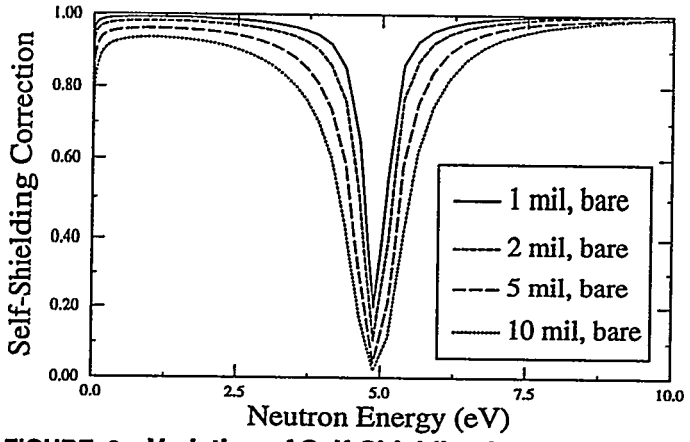

FIGURE 2. Variation of Self-Shielding in Gold 4.9 eV Resonance For Different Foil Thicknesses

ever possible. In special low fluence environments [7], thick foils may be required to give realistic counting times.

Many activation foils have a strong thermal response. The thermal response usually comes from an (n,γ) cross section and has a 1/v energy-dependence. In addition to this thermal 1/v component of the cross section, many dosimetry sensors have large resonance regions. By using cadmium covers (see Section III), the 1/v thermal response can be reduced so that the primary response of the sensor is in the region of a resonance. Figure 2 shows the self-shielding correction factor for the $^{197}Au(n,\gamma)^{198}Au$ 4.9 eV resonance. Since the resonance structure varies for each isotope, it is often useful to use several resonance reactions and different cover materials as sensors to characterize a neutron spectrum.

The literature [8, 9, 10, 11] notes that other reactions, such as $^{59}Co(n,\gamma)^{60}Co$, $^{164}Dy(n,\gamma)^{165}Dy$, and $^{115}In(n,\gamma)^{116}In$, can also have significant self-shielding in the region of cross-section resonances. Figure 3 shows the energy-dependent correction factor for some commercially available dosimetry sensors whose typical application is to yield spectral information in the resonance region. The figure shows an enlargement of the resonance region self-shielding corrections. Correction factors in the thermal and high energy region exhibit features similar to that shown in Figure 1 for gold.

The correction factors in Figures 1-3 were obtained by using Monte Carlo transport techniques to model the sensor geometry. The methodology and sensor geometries are discussed in Section IV. Several different shapes can be seen in the response correction factors in Figures 1-3. The large gold 4.9 eV resonance is a case where absorption is the dominant neutron interaction process and one sees a classic self-shielding correction. The serpentine correction factors for $^{59}Co(n,\gamma)^{60}Co$ and $^{55}Mn(n,\gamma)^{56}Mn$ occur when there is a significant scattering cross section in the region of the resonance. Here, the high-energy enhancement is the result of a neutron scattering down into the resonance energy region. For incident neutron energies at or below the peak energy of the resonance, the scattering processes result in a decreased effective neutron (n,γ) response. The large peak in the $^{23}Na(n,\gamma)^{24}Na$ reaction near 40 keV in Figure 3 shows a case where a trough between two large resonances is filled-in due to neutron scattering.

Dosimetry quality dilute foils are not commonly used for materials other than gold. Dilute cobalt wire is available from the National Institute of Standards and Technology (NIST), but due to the long half life of the ^{60}Co product, high-irradiation fluences may be required to get good counting statistics. Dilute solutions of other materials can be prepared for activation studies, but because of the counting difficulties and liquid waste disposal issues this is not a common practice.

For information on self-shielding correction factors, the typical user refers to community standards, such as ASTM E-262 [12]. Here the user is told to use his/her knowledge of the spectrum to estimate the correction to a measured activity. This is not a very satisfactory approach when the activity is being used to determine the spectrum. However, the method can be applied when the total sensor response is in a region where the physics

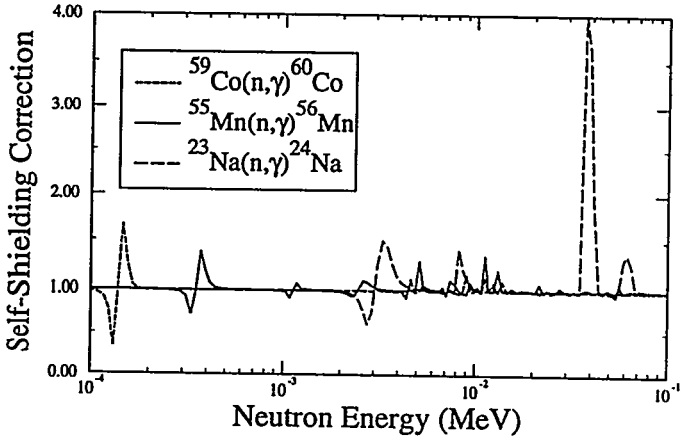

FIGURE 3. Self-Shielding in the Resonance Region

of the neutron scattering gives some guidance on the spectral shape, such as a Maxwellian shape in the thermal region or a $1/E^{1-\alpha}$ behavior [13] in the resonance region of a well moderated beam. But if the sensor response is divided between a prominent resonance and another region, this approach fails.

The most accurate treatment of resonance self-shielding for reactor dosimetry is developed in Reference 14. In this methodology individual resonance correction factors are analytically modeled with integral transport theory using a narrow resonance approximation for each dosimetry foil. The individual resonance corrections factors are then grouped, weighted with a 1/E spectrum within an energy group, and combined into a single foil correction factor weighting the energy-grouped correction factors with a calculated multigroup approximation of the reactor spectrum. This approach has been used to compare calculated-to-experiment (C/E) ratios for foil activation. There is no indication in the literature that the corrected foil activities were ever used to improve an experimental spectrum characterization. However, these multigroup self-shielding correction factors could be applied to the multigroup cross sections used in least-square-based spectrum determination codes.

When an iterative "unfold" technique is used, a commonly used approach, called the outer iteration technique [15], is to use the structure in the dosimetry cross sections and a smoothness criteria on the neutron spectrum to help fix the neutron trial spectrum. Self-shielding in a resonance region, even if it does not represent a significant part of the integrated sensor response, will interfere with this outer iteration approach due to the shape inaccuracies in the response function. Errors of 4%-5% in the measured activities for cross sections that exhibit strong resonance structures will result in unphysical features in "unfolded" spectra.

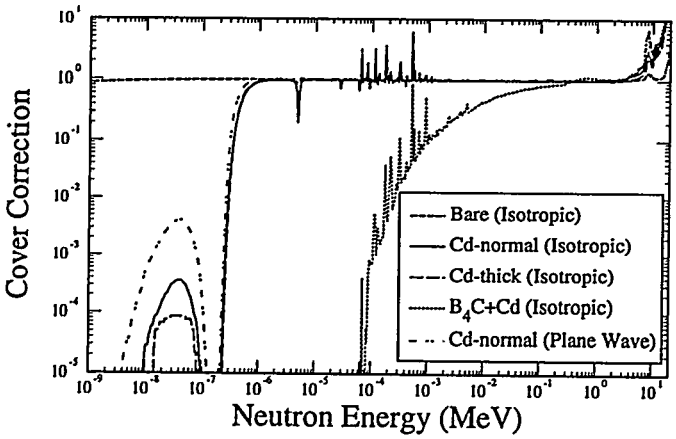

FIGURE 4. Effect of Various Covers on a 1-mil Gold Foil

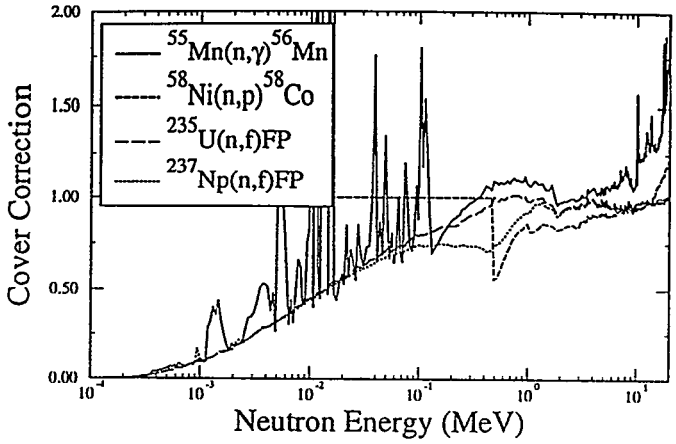

FIGURE 5. Effect of Neutron Scattering in a B_4C+Cd Cover

III. EFFECT OF COVERS

Cadmium and boron covers are used to suppress the thermal response of a dosimetry sensor. Cadmium is typically used with gold, indium, dysprosium, and other sensors where the thermal response is predominant. Cadmium provides good attenuation for neutrons with energies below 0.2 eV. Boron, typically in the form of B_4C with 92% enriched ^{10}B, provides neutron absorption over a broader energy range from its 1/v absorption cross section. Boron is almost always used as a cover for fission foils and can be useful with resonance-region reactions such as $^{55}Mn(n,\gamma)^{56}Mn$ and $^{45}Sc(n,\gamma)^{46}Sc$. Experimenters have to be aware that boron covers can shift the response of some well characterized foils into an energy region where the cross section is not as well known. Least squares codes take this into account by using the cross section uncertainty information. Iterative "unfold" codes can produce anomalous behavior if the sensor response is not well characterized in the region of primary response.

When covers are employed, users typically model the sensor response by applying an energy-dependent exponential attenuation term, based on the material neutron absorption cross section, to the dosimetry reaction cross section. While this approach is a good first-order correction, it ignores the role of neutron scattering on the high energy part of the sensor response. There have been some attempts in the literature to calculate and measure [16, 4] the spectrum-averaged downscattering effect in individual threshold reaction foils, such as $^{58}Ni(n,p)^{58}Co$ and $^{237}Np(n,f)FP$. Figure 4 shows the energy-dependent correction factor for several different cover materials and irradiation geometries (details of the configuration are described in Section IV.B) for a 1-mil gold foil.

Figure 5 shows several examples of the Monte Carlo modeling (described in Section IV) of the B_4C-covered sensor response correction factor. Since this correction factor is designed for use in existing spectrum "unfold" codes in place of the conven-

tional exponential attenuation model for covers, threshold reactions such as $^{58}Ni(n,p)^{58}Co$ show a correction factor of unity below the reaction threshold energy. The low energy attenuation/absorption by the B_4C cover is modeled fairly well by the conventional exponential attenuation. However, when neutrons scatter, the neutron energy is degraded. The scattered neutron has a lower effective energy. This can result in either an increase or a decrease in the effective sensor cross section depending on whether the cross section is decreasing or increasing in the energy region. This scattering effect is important at higher neutron energies (> 0.1 MeV) and near cross-section resonances. This effect is not modeled in the conventional approach.

IV. SNL COVER METHODOLOGY

A *Approach*

The optimal approach to calculating the appropriate response function for a specific dosimetry sensor is to use adjoint radiation transport techniques [17]. The adjoint source term is the dosimetry cross section, and the source is sampled over the same material volume that is used for the activity measurement. The effective sensor response function is the adjoint current scored on the outer sensor surface where the neutron spectrum is being determined.

At the Sandia National Laboratories (SNL) Radiation Metrology Laboratory (RML), the standard fission foil sensor consists of a stacked set of foils in a cylindrical cadmium cover and surrounded by a nearly spherical B_4C ball. We desired to treat covers and self-shielding with the highest possible fidelity. The sensor geometry necessitates the use of a 3D radiation transport code. Since we desire a fine resolution for the self-shielding of the resonance structures in the response function, a point cross-section transport code is required. The only code that meets these constraints (Monte Carlo, 3D, adjoint, point cross section) is ANTE [18]. However, the ANTE code is no longer actively supported and only has ENDF/B-IV vintage cross sections. Processing codes do not exist for preparing a new state-of-the-art cross section library for ANTE. The MCNP [19] radiation transport code can not be used since, although it is a general geometry point cross-section code when used in the forward mode, the MCNP adjoint implementation uses multigroup cross sections.

Due to the lack of an adequate high fidelity adjoint code, we were forced to use a brute force method rather than the more elegant adjoint methodology. Instead of a single adjoint calculation for each sensor configuration, a series of 640 monoenergetic forward calculations were performed with the MCNP (version 4A) code. The Perl 5 [20] scripting language was used along with a template file of the sensor configuration to automate the preparation of the MCNP input files and the processing of the results. This approach is computationally very inefficient, but requires very few man-hours to implement. Each calculation used the MCNP point cross sections for transport purposes, but used a 640 energy bin representation of the dosimetry cross section from Reference 5 to score the sensor response. The computations presented in this paper were performed using a SUN Sparc 20 while executing the Perl script and MCNP code in the background mode to avoid impacting other jobs.

B. *Implementation*

The title of this article addresses an "exact" treatment of self-shielding and covers. The methodology utilized supports an "exact" calculation. The implementation is as "exact" as the user desires for efficient application. Approximations in the methodology can occur in several areas. These areas and the current implementation approaches are discussed in the following bullets:

- Selection of an energy grid. We have chosen to use a high-resolution, 640 SAND-II multigroup representation [21] of each effective cross section since this is the finest grid used in any popular spectrum "unfold" code. This means that we perform 640 forward calculations for every sensor/geometry combination. Each calculation uniformly samples the energy within one SAND-II energy bin. Any coarser energy grid is inconsistent with modeling the self-shielding effects. A finer energy grid could not be utilized by any of the current spectrum "unfold" codes.
- Modeling of the sensor geometry. We model the detailed sensor geometry. This is why a general geometry 3D Monte Carlo code is required. The geometry of the boron balls and cadmium pillboxes is described in Reference 4. Tables 1 and 2 provide a brief description of the configurations modeled in this study. Due to space limitations in this paper, a more detailed description of the sensor geometries will be provided in a separate Sandia National Laboratories report. This laboratory report will accompany the distribution of the self-shielding correction factors as part of version 2 of the SNL-SAND-II code. Details on this distribution are provided in Section IV part C.
- Modeling of the angular distribution of incident neutrons. Current angular distribution models include a plane wave incident perpendicular to the sensor face (this represents a far-field sensor placement) and an isotropic distribution (this represents sensors exposed in a reactor central core and far-field sensors dominated by thermal neutron response). The isotropic distribution is implemented by using an isotropic inward-directed spherical shell source surrounding the sensor at a radius ten times the largest sensor dimension. Source biasing techniques are used to ensure efficient sampling. For a nonpoint sensor this is not exactly an isotropic source, but it is a very good approximation. The plane wave and isotropic angular distributions represent extremes in the incident neutron angular distributions and can be used to quantify the importance of the angular modeling for any spectrum characterization. For

the cases studied, the effect of the angular distribution appears to be small.

Higher fidelity modeling of the angular distributions could be implemented by using angular distributions computed by Monte Carlo modeling of the actual reactor and containment structures (a kiva at SNL) and scoring energy/angular distributions at the sensor locations. The energy/angular distributions could be interfaced with the Perl script and the template file to model the effective sensor cross section. Plans are underway to use a detailed SPR-III model [22] to compute such energy/angle distributions and to quantify the effect of this angular distribution approximation for far-field sensors (120 in. and 80 in. leakage spectra at SPR-III).

- Criteria for statistical convergence. The number of Monte Carlo histories varied from 50,000 to 5,000,000 based on the cover absorption cross section in the particular energy region. Some simple rules were programmed into the Perl script to implement the selection of the number of histories. At high energies, the number of histories was sufficient to provide statistical uncertainties less than 2% and to pass at least 8 of the 10 statistical tests built into the MCNP4a code. In areas of high absorption (e.g., below 0.2 eV with a cadmium cover), an attenuation factor of 10^{-5} could occur. In these cases, even 5,000,000 histories and exponential weighting of the transport process could not ensure good statistics. However, these areas of high absorption also do not play a significant role in the sensor response to any actual reactor spectra.

The authors have calculated sensor response functions for over 80 sensor configurations. Configurations include isotropic and plane beam geometries, various dosimetry reactions, foil thicknesses, and foil stacking geometries. The SNL-SAND-II code has been modified so that the normal cover designation can be replaced by a code word "covr" and a two-word description of the sensor geometry. The two-word description consists of a four character cover and a four character configuration descriptor. The descriptors are limited to four characters to preserve compatibility with the SAND-II VIF input format. Tables 1 and 2 define the various descriptors currently implemented.

Table 1. Definition of Cover Descriptors

Cover Descriptor	Description
bare	a bare foil.
cdnm	a foil in a normal cadmium cover with a thickness of 23.1 mils on the source side and 19.8 mils on the back side and a density of 8.65 g/cm^3.
cdtk	a foil in a thick cadmium cover with a thickness of 30.3 mils on the source side and 30 mils on the back side and a density of 8.65 g/cm^3.
b4c	a foil fielded in a 1.03-cm-thick boron shell with a B_4C composition, a 91.67% ^{10}B boron enrichment, and an inner radius of 1.35 cm.
fiss	a foil fielded in a thick cadmium cover and enclosed in a boron ball (cdtk + b4c covers).

Table 2. Definition of Configuration Descriptors

Configuration Descriptor		Description
Isotropic	Plane Wave	
mil1	bmm1	A 1-mil-thick disk-shaped foil.
mil2	bmm2	A 2-mil-thick disk-shaped foil.
mil5	bmm5	A 5-mil-thick disk-shaped foil.
milx	bmmx	A 10-mil-thick disk-shaped foil.
ml3x	bm3x	A 30-mil-thick disk-shaped foil.
dil5	bil5	A 5-mil-thick disk-shaped dilute foil. The dilution level is 0.1143% (weight) in an aluminum matrix.
wcu2	bcu2	A 2-mil-thick disk-shaped foil. The material is present at a 81% (atom) level in a copper matrix.
pelt	bplt	A NaCl pellet configuration with a radius of 157 mil, a thickness of 107 mil, and a density of 2.165 g/cm^3.
sulf	bslf	A sulfur pellet configuration with a radius of 250 mil, a thickness of 150 mil, and a density of 1.79 g/cm^3.
void	bvod	An infinitely dilute foil.
rmle	brme	The rmleu fission foil, a 93% (atom) enriched ^{235}U foil with ^{234}U, ^{236}U, and ^{238}U contaminants.
rmld	brmd	The rmldu fission foil, a depleted uranium foil with 99.79% (atom) ^{238}U, and 0.205% ^{235}U.
rmlp	brmp	The rmlpu fission foil, a plutonium foil with 86.9965% (atom) ^{239}Pu and modeled contaminants of ^{238}Pu, ^{240}Pu, ^{241}Pu, ^{242}Pu, ^{235}U, and ^{237}Np.
skle	bske	The rmleu foil in the normal position in a SNL standard stacked fission foil configuration. The stacking order from the source side back is Ni, rmldu, ^{237}Np, rmlpu, rmleu. Cadmium disks with a thickness of 30 mils are used between foils to reduce the buildup of any thermal neutrons.
skld	bskd	The rmldu foil in the normal position in a SNL standard stacked fission foil configuration.
skpu	bskp	The rmlpu foil in the normal position in a SNL standard stacked fission foil configuration.
sknp	bsnp	The ^{237}Np foil in the normal position in a SNL standard stacked fission foil configuration.
skni	bsni	The nickel monitor foil in the normal position in a SNL standard stacked fission foil configuration.

The dosimetry reactions modeled in these configurations include $^{109}Ag(n,\gamma)^{110}Ag$, $^{197}Au(n,\gamma)^{198}Au$, $^{59}Co(n,\gamma)^{60}Co$, $^{63}Cu(n,\gamma)^{64}Cu$, $^{115}In(n,\gamma)^{116m}In$, $^{54}Fe(n,p)^{54}Mn$, $^{56}Fe(n,p)^{56}Mn$, $^{24}Mg(n,p)^{24}Na$, $^{55}Mn(n,\gamma)^{56}Mn$, $^{98}Mo(n,\gamma)^{99}Mo$, $^{23}Na(n,\gamma)^{24}Na$, $^{58}Ni(n,p)^{58}Co$, $^{32}S(n,p)^{32}P$, $^{45}Sc(n,\gamma)^{46}Sc$, $^{46}Ti(n,p)^{46}Sc$, $^{47}Ti(n,p)^{47}Sc$, $^{48}Ti(n,p)^{48}Sc$, $^{237}Np(n,f)FP$, $^{239}Pu(n,f)FP$, $^{235}U(n,f)FP$, $^{238}U(n,f)FP$, rmleu, rmldu, and rmlpu. The rml"xx" sensors (where "xx" can be "eu", "du", or "pu") are fission foils that include a complete description of contaminate materials. The designators "eu", "du", and "pu" stand for "enriched uranium", "depleted uranium", and "plutonium" respectively. A complete description of these fission foil compositions can be found in Reference 5, Sections 5.56 through 5.68.

All possible permutations of the foil, geometry, and configurations parameters have not been modeled at this time. The currently implemented models have been restricted to sensor configurations in use at SNL or being used for studies of the systematics of the cover effects. The Perl scripts and MCNP template files exist to rapidly characterize elements of this matrix that are in use at other reactor facilities.

C. Availability

These resulting response functions have been interfaced with the SNL-SAND-II code [3] as a complement to the exponential attenuation models. The response functions will soon be distributed to the general dosimetry community through the Oak Ridge National Laboratory Radiation Shielding Information Center with the release of version 2 of the SNL-SAND-II code.

The response functions have also been interfaced to the SNL version of the LSL code. Generalized least squares approaches to spectrum "adjustment" require covariance matrices for the response functions. The response function covariance matrices will be affected by the use of these correction functions. In fact, serious cross reaction correlations will likely be introduced for sensors with a common cover. These same issues apply to the current use of exponential-attenuation cover models in least squares codes. Since a covariance matrix is available for the primary absorption cross section in boron, it should be possible to provide correction factors to the response covariance matrices, at least to a first order approximation, using an exponential-attenuation model.

V. APPLICATION IN SPECTRUM CHARACTERIZATIONS

Table 3 shows the effect of the modeling approach on the calculated sensor response for several reactions on two fission reactor spectra, one very hard and one very soft. The reactor spectra represent a soft pool-type spectrum and an artificially hardened (by enclosure in a boral box) fast-burst spectrum [23]. In fast-burst reactors, with a hard spectrum, the use of B_4C covers can result in the most significant part of the response occurring at high energies where scattering effects are important. Thus, for a hard spectrum, the threshold reactions, such as $^{58}Ni(n,p)^{58}Co$ and $^{32}S(n,p)^{32}P$, show bigger differences from the exponential modeling than nonthreshold reactions such as $^{55}Mn(n,\gamma)^{56}Mn$ and $^{45}Sc(n,\gamma)^{46}Sc$.

The rmldu depleted uranium exponential-attenuation factor from Table 3 is 0.492 for the soft ACF9 spectrum and 0.950 for the hard BBALL11 spectrum. This may strike the reader as a very large difference for a threshold reaction that shouldn't be affected by the thermal component of the neutron spectrum. The table entries are correct. This large difference is the result of the ^{235}U contaminant in the depleted uranium. Even though the ^{235}U contaminant level is only 0.205% (atom), the large ^{235}U thermal cross section and the soft ACF9 spectrum result in this contaminant producing about half of the fissions in a bare foil configuration [5]. This sensitivity to contaminants is one of the reasons fission foils are routinely fielded in boron covers. In a boron cover the ^{235}U fission fraction is reduced to 0.2% for the ACF9 spectrum. The rmlpu foil is composed of 87% (atom) ^{239}Pu, 11.6% (atom) contamination of ^{240}Pu, and other small levels of plutonium isotopes. The ^{240}Pu contaminant is responsible for about 6% of the fissions in a hard spectrum and in a boron-covered configuration. However, a bare rmlpu foil in a soft ACF9 spectrum only has 0.08% contribution from the ^{240}Pu contaminant. These two examples show why an important part of the sensor modeling for fission foils is a correct representation of the fissionable contaminants.

Table 3 also shows measured sensor ratios for the hard spectrum. The BBALL11 environment was characterized using the normal set of dosimetry sensors with the SAND-II code. Then several irradiations were done to characterize the effect of the boron ball on individual dosimetry sensors. A Cd-covered (cdnm) dosimetry foil and one in a cadmium cover inside a boron ball (fiss) were simultaneously exposed along with a nickel monitor foil. The foils were separated by a small distance (~ 6 inches) so that scattered neutrons from the boron ball would not affect the Cd-covered foil. The 30 in. leakage location was chosen for this experiment so that there would be a negligible fluence gradient between these two foil positions but enough separation to prevent the boron ball from modifying the free-field neutron spectrum. The measured ratios in column 3 of Table 3 agree fairly well with the "transport correction" modeling. This agreement (measurement to calculation) could probably be improved if all sensor data, including B_4C covered sensors, are used to better characterize the BBALL11 spectrum.

Table 3 shows transport correction factors calculated with two different models. The entries in parenthesis in column 4 correspond to fielding a single unstacked sensor. However, most fast-burst reactor experimenters have traditionally fielded stacked fission foils within a boron ball. The numbers without the parenthesis represent the stacked configuration. Concern

about dosimeter placement and the necessity of avoiding large sensor configurations that could perturb the free-field neutron spectrum do not generally permit fielding multiple boron balls in a single irradiation. Boron ball configurations are generally irradiated separate from bare and cadmium-covered foils to avoid perturbing the bare foil response. If unstacked fission foils were used, a typical spectrum characterization would require five irradiations rather than the current two irradiations. Combining activities from separate irradiation steps increases the uncertainty of the activities and introduces correlations in the measurements that are difficult to characterize and apply during the spectrum determination.

The fission foil stacking corrections for nonthreshold reactions (such as rmleu and rmlpu) shown in Table 3 are larger than had been expected. Additional experiments at SNL and at White Sands Missile Range have reinforced the concern about the foil stacking corrections. Work is currently underway to investigate other stacking configurations. Future spectrum characterizations at SNL will probably use separate fission foil irradiations until the sensitivity to stacking configuration is better understood.

VI. CONCLUSION

This paper shows that the conventional treatment of dosimetry covers can distort the shape of the effective response function and cause changes in the spectrum-averaged cross sections of 4%-10%. The relative measurement uncertainty associated with most dosimetry sensors used in spectrum determinations

Table 3. Effect of Cover Treatment of the Spectrum-Averaged Cross Section Inside a B_4C+Cd Cover

Spectrum [Ref. 23]	Reaction	Measured Correction Factor (fiss cover/Cd cover)	Modeling Methodology (fiss cover/Cd cover)		
			Transport Correction[1]	Exponential Attenuation	Modeling Difference[1] (%)
ACF9, ACRR Central Cavity	$^{58}Ni(n,p)^{58}Co$	NA	0.874/(0.885)	0.957	-9.5%/(-8.1%)
	RMLEU		0.0198/(0.0189)	0.0210	-6.3%/(-11.1%)
	$^{237}Np(n,f)FP$		0.914/(0.910)	0.9445	-3.3%/(-3.8%)
	RMLDU		0.454/(0.462)	0.492	-8.4%/(-6.5%)
	RMLPU		0.0113/(0.0106)	0.0114	-0.9%/(-7.5%)
	$^{55}Mn(n,\gamma)^{56}Mn$		0.0337	0.0397	-0.6%
	$^{45}Sc(n,\gamma)^{46}Sc$		0.0407	0.0404	-0.7%
	$^{32}S(n,p)^{32}P$		0.885	0.956	-8.0%
BBALL11, Inside Boral Box 30" From SPR-III Core	$^{58}Ni(n,p)^{58}Co$	0.894	0.877/(0.886)	0.957	-9.1%/(-8.0%)
	RMLEU	0.694	0.707/(0.685)	0.711	-5.7%/(-3.8%)
	$^{237}Np(n,f)FP$	0.875	0.919/(0.917)	0.957	-4.1%/(-4.4%)
	RMLDU	0.882	0.873/(0.889)	0.950	-8.8%/(-6.9%)
	RMLPU	0.747	0.731/(0.693)	0.720	1.5%/(-3.9%)
	$^{55}Mn(n,\gamma)^{56}Mn$	tbd	0.170	0.166	+2.4%
	$^{45}Sc(n,\gamma)^{46}Sc$	tbd	0.490	0.469	+4.3%
	$^{32}S(n,p)^{32}P$	0.897	0.889	0.957	-7.6%
	$^{54}Fe(n,p)^{54}Mn$	0.900	0.909	0.957	-5.3%
	$^{56}Fe(n,p)^{56}Mn$	0.897	0.9.05	0.964	-6.58%
	$^{47}Ti(n,p)^{47}Sc$	0.916	0.914	0.957	-4.7%
	$^{24}Mg(n,\alpha)^{24}Na$	0.902	0.901	0.965	-7.1%
	$^{27}Al(n,\alpha)^{24}Na$	0.910	0.918	0.966	-5.2%

[1]Sensor modeling includes foil stacking for fission foils and nickel monitors and the assumption of an isotropic angular distribution. The numbers in parenthesis correspond to fielding a single unstacked sensor. All other foils (nonfission and nonnickel) are typically fielded without foil stacking.

is from 2%-3%. The uncertainty in the spectrum-averaged activity due to the knowledge of dosimetry-quality cross section is often from 3%-5%. Thus the improved modeling procedure outlined in this paper will significantly improve the agreement between dosimetry sensors fielded in well-characterized environments. The improved modeling of self-shielding in this approach allows the use of thick thermal sensors when it is not feasible to use dilute forms (due to availability or low count rates). In addition, this more exact modeling of the effects of cover materials opens the possibility of using B_4C covers on more sensors to shift their response to higher energies and to provide better overall energy coverage by a sensor set. The results of this study are being made available to the general dosimetry community and can be readily applied to any spectrum determination code.

VII. REFERENCES

[1] W. Stallman, LSL-M2: A Computer Program for Least-Squares Logarithmic Adjustment of Neutron Spectra, NUREG/CR-4349, ORNL/TM-9933, Oak Ridge National Laboratory, Oak Ridge, Tenn., March 1985.

[2] W. N. McElroy, S. Berg, T. Crockett, and R. Hawkins, A Computer-Automated Iterative Method for Neutron Flux Spectral Determination by Foil Activation, AFWL-TR-67-41, Vol. 1, Air Force Weapons Laboratory, Kirtland AFB, Albuquerque, New Mexico, July 1967.

[3] P. J. Griffin, J. G. Kelly, J. W. VanDenburg, User's Manual for SNL-SAND-II Code, SAND93-3957, Sandia National Laboratories, Albuquerque, New Mexico, 1994.

[4] J. G. Kelly, D. W. Vehar, Measurement of Neutron Spectra in Varied Environments by the Foil-Activation Method With Arbitrary Trials, SAND87-1330, Sandia National Laboratories, Albuquerque, NM, December 1987.

[5] P. J. Griffin, J. G. Kelly, T. F. Luera, SNL RML Recommended Dosimetry Cross Section Compendium, SAND92-0094, Sandia National Laboratories, Albuquerque, New Mexico, 1993.

[6] G. Borchardt, "Gadolinium Filter for Thermal Neutrons," Atomkerenergie, Vol. 15, p. 311, 1970.

[7] T. W. L. Sanford, L. J. Lorence, J. A. Halbleib, J. G. Kelly, P. J. Griffin, J. W. Poukey, W. H. McAtee, R. C. Mock, "Photoneutron Production Using Bremsstrahlung from the 14-TW Pulsed-Power HERMES-III Electron Accelerator," Nuclear Science and Engineering, Vol. 114, No. 3, pp. 190-213, July, 1993.

[8] T. A. Eastwood, R. D. Werner, "Resonance and Thermal Neutron Self-Shielding in Cobalt Foils and Wires," Nuclear Science and Engineering, Vol. 13, pp. 385-390, 1962.

[9] T. B. Ryves, "A New Thermal Neutron Flux Convention," Metrologia, Vol. 5, No. 4, 1969.

[10] T. L. Gallagher, "Foil Depression Factors for Indium Disk Detectors (Letter to the Editor)," Nuclear Science and Engineering, Vol. 3, No. 1, pp. 110-112, 1958.

[11] T. B. Ryves, K. J. Zieba, "The Resonance Integrals of ^{63}Cu, ^{65}Cu, ^{107}Ag, ^{159}Tb, ^{164}Dy, and ^{165}Ho," Journal of Physics A, Vol. 7, No. 18, pp. 2318-2332, 1974.

[12] "Standard Test Method for Determining Thermal Neutron Reaction and Fluence Rates by Radioactivation Techniques," Designation E 262-86, Annual Book of ASTM Standards, Vol. 12.02, 1994.

[13] A. Ahmad, "Analysis and Evaluation of Thermal and Resonance Neutron Activation Data," Ann. Nucl. Energy, Vol. 10, pp. 41-50, 1983.

[14] S. C. Mo, K. O. Ott, "Resonance Self-Shielding Corrections for Detector Foils in Fast Neutron Spectra," Nuclear Science and Engineering, Vol. 95, pp. 214-224, 1987.

[15] J. G. Kelly, "Neutron Spectrum Adjustment with SAND-II Using Arbitrary Trial Functions," Reactor Dosimetry Methods, Applications, and Standardization, ASTM STP 1001, Harry Farrar IV and E. P. Lippincott, Eds., American Society for Testing and Materials, Philadelphia, pp. 460-468, 1989.

[16] J. T. Harvey, J. L. Meason, "Neutron Attenuation Due to Boron-10 Shields (Technical Notes)," Nuclear Science and Engineering, Vol. 67, pp. 343-344, 1978.

[17] C. O. Slater, J. C. Robinson, "Forward-Adjoint Coupling as a Means of Solving Three-Dimensional Deep-Penetration Transport Problems," Nuclear Science and Engineering, Vol. 53, pp. 332-337, 1974.

[18] M. O. Cohen, M. Beer, ANTE-3 - A FORTRAN Computer Code for the Solution of the Adjoint Neutron Transport Equation by Monte Carlo Techniques, MR-7028, DNA-2988F, Mathematical Applications Group, Inc., Elmsford, NY, Oct. 1972.

[19] J. Briesmeister, Editor, MCNP - A General Monte Carlo N-Particle Transport Code, Version 4A, LA-12625-M, UC 705 and UC 700, Los Alamos National Laboratory, Los Alamos, NM, November 1993.

[20] L. Wall, R. L. Schwartz, Programming Perl, A Nutshell Handbook, O'Reilly & Associates, Inc., Sebastopol, CA, March 1992.

[21] R. E. MacFarlane, D. W. Muir, R. M. Boicourt, The NJOY Nuclear Data Processing System, Volume 1: User's Manual, LA-9303-M, ENDF-324, Los Alamos National Laboratory, Los Alamos, NM, May 1982.

[22] J. G. Kelly, P. J. Griffin, W. C. Fan, "Benchmarking the Sandia Pulsed Reactor III Cavity Neutron Spectrum for Electronic Parts Calibration and Testing," IEEE Trans. Nucl. Science, Vol. NS-40, No. 6, pp. 1418-1425, Dec. 1993.

[23] P. J. Griffin, J. G. Kelly, D. W. Vehar, Updated Neutron Spectrum Characterization of SNL Baseline Reactor Environments: Vol. 1: Characterization, SAND93-2554, Sandia National Laboratories, Albuquerque, New Mexico, 1994.